Hindawi
Wireless Communications and Mobile Computing
Volume 2022, Article ID 1400114, 10 pages
https://doi.org/10.1155/2022/1400114

Research Article

Influence of Sublevel Unloading Excavation with Deep Consideration of the Superposition Effect on Deformation of an Existing Tunnel under an Intelligent Geotechnical Concept

Xiangling Tao,[1,2,3] **Pinzhi Luan**,[2] **Jinrong Ma**,[2] **and Weihua Song**[4]

[1]*College of Innovation and Entrepreneurship, Jiangsu Vocational Institute of Architectural Technology, Xuzhou 221116, China*
[2]*State Key Laboratory for Geomechanics and Deep Underground Engineering, China University of Mining and Technology, Xuzhou 221116, China*
[3]*Anhui Huizhou Geology Security Institute Co. Ltd., Hefei 230000, China*
[4]*Xuzhou New Town State-Owned Assets Management Co. Ltd., China*

Correspondence should be addressed to Xiangling Tao; taoxl@cumt.edu.cn

Received 29 November 2021; Revised 17 December 2021; Accepted 22 December 2021; Published 31 January 2022

Academic Editor: Liqin Shi

Copyright © 2022 Xiangling Tao et al. This is an open access article distributed under the Creative Commons Attribution License, which permits unrestricted use, distribution, and reproduction in any medium, provided the original work is properly cited.

The construction of a deep and large foundation will inevitably impose stress and deformation on the existing shield tunnel structure. Based on the two-stage analysis and the Pasternak foundation beam model, the analytical solution for the existing tunnel deformation is derived by taking the grouting pressure and water buoyancy into account in the total tunnel deformation. Using FLAC 3D software, based on the soil-structure interaction model, the variation law of the tunnel uplift value under partition excavation of the foundation pit is studied and the variation law of the stress field and displacement field of the tunnel under the MJS method is analyzed and compared. The results of this paper are worthy of reference for similar projects.

1. Introduction

With the rapid construction of urban underground space development, it is often encountered that the new foundation pit or tunnel project is adjacent to the existing tunnel construction. Therefore, the deformation analysis of the built operation tunnel by underground space unloading development has become a key problem to be solved in projects and scholars are gradually keen on analyzing the influence of excavation on existing tunnels.

The unloading of foundation pit excavation will cause the change of the displacement field and stress field of the underlying shield tunnel. When the vertical displacement or lateral convergence deformation of the shield is large, it will seriously affect the safe use and operation of the existing tunnel [1–5]. At present, many scholars have used theoretical calculation [6–8], numerical simulation [9–12], and measured analysis [13, 14] to conduct in-depth analysis on the deformation of the underlying tunnel caused by foundation pit excavation under different geological conditions or construction schemes. In addition, many factors are also considered in the research on the mechanism of stress and displacement of a tunnel caused by loading or unloading. Zhang et al. [15] considered the role of the foundation pit supporting structure, established the additional confining pressure variation model of adjacent shield tunnels considering the influence of longitudinal deformation, and obtained the variation law of the influence of foundation pit excavation on the lateral force of shield tunnels.

Jiang [16] introduced the rheological deformation of soil in the viscoelastic-plastic theoretical model and analyzed the deformation law of existing tunnels under different relative distances, excavation areas, and construction procedures in the process of foundation pit excavation. Zhang et al. [17] considered the dewatering effect of the foundation pit and obtained the theoretical calculation formula of additional stress and vertical deformation of the underlying existing tunnel caused by upper excavation and dewatering. Hefny

and Chua [18] used PLAXIS software combined with specific working conditions to study the influence of the new tunnel close crossing construction on the existing tunnel. Tao et al. [19] took the segment floating of Q3 clay subway tunnel excavation in Xuzhou as the research object and obtained the analytical solution of segment floating caused by shield tunnel excavation. Liang et al. [20] considered the bending and shear effects of the shield tunnel in solving the tunnel deformation caused by foundation pit excavation and compared it with the simulation results and measured values to verify the correctness of the theoretical solution. Tan et al. [21] analyzed the influence of partition excavation of foundation pit on subway tunnel around foundation pit from the perspective of engineering measured data under sensitive geological conditions of hard clay. Sun et al. [22] studied the deformation law of tunnel under different excavation methods of foundation pit. Zhang et al. [23] simplified the existing shield tunnel as a Timoshenko beam placed on the Pasternak foundation, and the longitudinal deformation formula of the existing shield tunnel induced by ground surcharge was derived. In summary, the existing research considers many factors when solving the stress and deformation law of the tunnel caused by the excavation of the foundation pit but few scholars consider the deformation caused by the excavation of the shield tunnel into the total deformation of the tunnel. Especially when the construction time of the foundation pit and the tunnel is close, the superposition construction effect of tunnel excavation and foundation pit excavation will cause large deformation of the tunnel. Therefore, based on the above research results, this paper analyzes the disturbance effect of the partition unloading of the foundation pit on the existing tunnel. Based on two-stage analysis method and Pasternak foundation beam model, a theoretical model of segment floating is established by spatializing the time axis. Solving the deformation law of the tunnel under superposition provides a more accurate calculation method of tunnel deformation for such projects. In addition, based on the overlapping passage project of Xuzhou Metro Line 2, this paper uses FLAC3D to carry out simulation and makes a more in-depth analysis of the internal force change and deformation mechanism of the tunnel under partition unloading, in order to provide a basis for the rational planning and construction of similar foundation pit projects.

2. Analytical Solution of Tunnel Vertical Deformation Caused by Excavation Unloading

2.1. Calculation Method of Additional Stress of the Tunnel Structure Caused by Excavation. Since the excavation time of the foundation pit is after the completion of tunnel construction, the interaction between the two on tunnel deformation is weak, so the tunnel deformation during tunnel construction and during foundation pit excavation is calculated separately in this paper. The excavation of the foundation pit in the existing subway tunnel belongs to the internal unloading effect of the soil. When calculating the tunnel deformation, the Mindlin elastic solution [24] can be used to calculate the vertical load acting on the tunnel structure first.

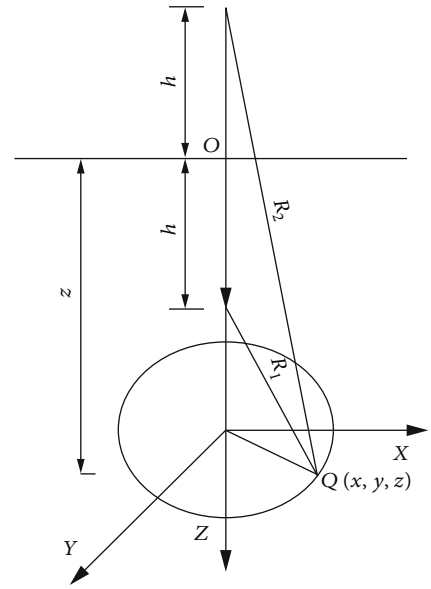

Figure 1: Mindlin solution diagram.

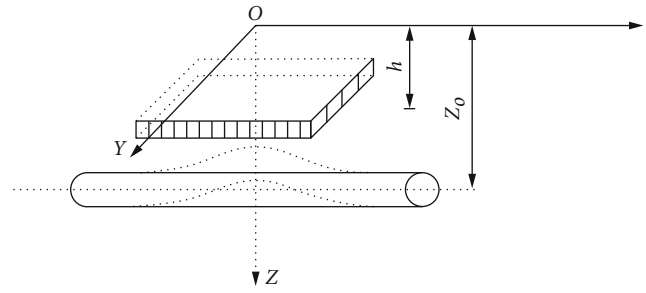

Figure 2: Mindlin diagram of the foundation pit above the tunnel.

Figure 1 shows the single-tunnel diagram of Mindlin solution. On this basis, we expanded it, combined with the actual working situation on the site, and conducted theoretical derivation again. Figure 2 shows the Mindlin solution diagram of the foundation pit above the tunnel.

When a point (ξ, η) acts on a concentrated force $pd\xi d\eta$ at depth h, the vertical additional stress at any point Q (x, y, z) in a semi-infinite elastic space soil is

$$\begin{aligned}\sigma_z = \frac{p}{8\pi(1-\nu)}\Bigg\{&(1-2\nu)(z_0-h)\iint_D \frac{d\xi d\eta}{R_1^3} \\ &+ 3(z_0-h)^3\iint_D \frac{d\xi d\eta}{R_1^5} - (1-2_\nu)(z_0-h)\iint_D \frac{d\xi d\eta}{R_2^3} \\ &+ \left[3(3-4_\nu)z_0(z_0+h)^2 - 3h(z_0+h)(5z_0-h)\right] \\ &\times \iint_D \frac{d\xi d\eta}{R_2^5} + 30hz_0(z_0+h)^3\iint_D \frac{d\xi d\eta}{R_2^7}\Bigg\},\end{aligned} \tag{1}$$

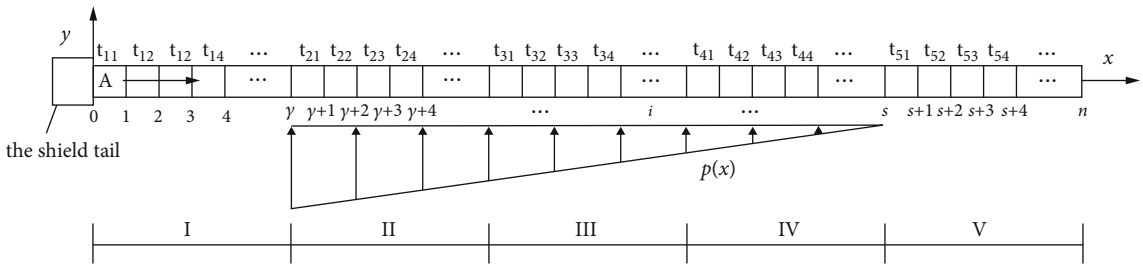

Figure 3: Calculation model of shield floating considering grouting pressure and water buoyancy.

with

$$R_1 = \sqrt{(x-\xi)^2 + (y-\eta)^2 + (z_0 - h)^2},$$
$$R_2 = \sqrt{(x-\xi)^2 + (y-\eta)^2 + (z_0 + h)^2}, \tag{2}$$

where ν is the Poisson's ratio, h is the excavation depth of the foundation pit, and z is the distance between the tunnel center line and the surface.

2.2. Solution of Vertical Deformation of the Tunnel Structure Caused by Foundation Pit Excavation. When calculating the vertical deformation at any position of the tunnel caused by the excavation of the foundation pit, considering the consistency with the calculation method of the floating amount caused by the tunnel construction, this paper uses the Pasternak foundation model to calculate the deformation of the existing tunnel under the additional load and the Pasternak foundation model can simulate the shear force between the soil springs and the continuity of the deformation; thus, the calculation results are more accurate. The stress of the tunnel is substituted into the model, and after a series of simplifications, the vertical deformation of the tunnel caused by the excavation of the foundation pit at any point can be obtained.

$$\omega(x) = e^{\alpha x}(C_1 \cos \beta x + C_2 \sin \beta x) + e^{-\alpha x}(C_3 \cos \beta x + C_4 \sin \beta x). \tag{3}$$

3. Analytical Solution of Tunnel Vertical Deformation considering Floating Factor

Figure 3 shows the upward deformation caused by grouting pressure, and water buoyancy often occurs during shield tunnel construction.

In the paper, the segment uplift is divided into five stages: (I) the ungrouted stage, (II) the fast uplift stage, (III) the slow uplift stage, (IV) the equilibrium stage, and (V) grout solidification.

According to the Pasternak foundation beam model, the differential equation of segment deflection caused by tunnel construction is

$$EI\frac{d^4y}{dx^4} - GB\frac{d^2y}{dx^2} + KBy = P(x), \tag{4}$$

where EI is the bending stiffness of the foundation beam (kN·m^2), y is the floating capacity (m), K is the foundation bed coefficient (kN/m^3), x is the longitudinal axis (m), G is the shear stiffness of foundation soil (kN/m), B is the width of the tube ring (m), P is buoyancy (kN), t is the time axis (m) after spatialization.

General solution of homogeneous equation of differential equation of torsion curve can be obtained according to formula (4)

$$y = e^{\alpha x}[C_1 \cos(\beta t) + C_2 \sin(\beta t)] + e^{-\alpha x}[C_3 \cos(\beta t) + C_4 \sin(\beta t)], \tag{5}$$

where C_1, C_2, C_3, and C_4 in the expression are constants to be determined and their values are determined by the boundary conditions. Since in equation (4), it is a special solution of equation (4). So the general solution of formula (4) is:

$$y = e^{\alpha t}[C_1 \cos(\beta t) + C_2 \sin(\beta t)] + e^{-\alpha x}[C_3 \cos(\beta t) + C_4 \sin(\beta t)] + \frac{at+b}{KB}. \tag{6}$$

The influence of the shield tail on point 0 is regarded as hinged support. Since the slurry has been solidified as a fixed end at point 3, the vertical displacement and bending moment of node 0 are equal to 0, the vertical displacement and rotation angle of node 3 are equal to 0, and the boundary conditions are

$$y_{10}|_{t=0} = 0,$$
$$y'_{10}|_{t=0} = 0,$$
$$y_{33}|_{t=3} = 0,$$
$$y'_{33}|_{t=3} = 0. \tag{7}$$

As shown in Figure 2, the connection points 1 and 2 of segment assembly (I), segment floating (II, III, and IV), and slurry (V) fully solidified; the deflection, rotation angle, bending moment, and shear force of point 1 of segment I, point 1 of segment II, point 2 of segment IV, and point 2

of segment V are the same, so the coordination equation between foundation beams is

$$\begin{aligned} y_{ij} &= y_{(i+1)j}, \\ \frac{dy_{ij}}{dt} &= \frac{dy_{(i+1)j}}{dt}, \\ E_i I_i \frac{d^2 y_{ij}}{dt^2} &= E_{i+1} I_{i+1} \frac{d^2 y_{(i+1)j}}{dt^2}, \\ E_i I_i \frac{d^3 y_{ij}}{dt^3} &= E_{i+1} I_{i+1} \frac{d^3 y_{(i+1)j}}{dt^3}, \end{aligned} \tag{8}$$

where y_{ij} is the deformation of the beam and j node in the i section (i is the beam element number, j is the beam node number, $i = j = 1, 2$). $E_i I_i$ is the equivalent stiffness of each segment. For formula (5), we obtain the 1st, 2nd, and 3rd derivatives, respectively, and then replace them with the boundary conditions and the coordination equation to obtain 12 square matrices:

$$[K][C] = [B]. \tag{9}$$

In the formula,

$$[K] = \begin{bmatrix} [K_{10}] & & & \\ [K_{11}] & -[K_{21}] & & \\ & -[K_{22}] & [K_{32}] & \\ & & & [K_{33}] \end{bmatrix},$$

$$[C] = [C_{11}\ C_{12}\ C_{13}\ C_{14}\ C_{21}\ C_{22}\ C_{23}\ C_{24}\ C_{31}\ C_{32}\ C_{33}\ C_{34}]^T,$$

$$[B] = \left[0 \quad 0 \quad \frac{at+b}{K_2 B_2} \quad \frac{a}{K_2 B_2} \quad 0 \quad 0 \quad \frac{at+b}{K_2 B_2} \quad \frac{a}{K_2 B_2} \quad 0 \quad 0 \quad 0 \quad 0\right]^T,$$

$$[K_{10}] = \begin{bmatrix} \gamma_{10} & \varepsilon_{10} & \lambda_{10} & \eta_{10} \\ \gamma'_{10} & \varepsilon'_{10} & \lambda'_{10} & \eta'_{10} \end{bmatrix},$$

$$[K_{11}] = \begin{bmatrix} \gamma_{11} & \varepsilon_{11} & \lambda_{11} & \eta_{11} \\ \gamma'_{11} & \varepsilon'_{11} & \lambda'_{11} & \eta'_{11} \\ \gamma''_{11} & \varepsilon''_{11} & \lambda''_{11} & \eta''_{11} \\ \gamma'''_{11} & \varepsilon'''_{11} & \lambda'''_{11} & \eta'''_{11} \end{bmatrix},$$

$$[K_{21}] = \begin{bmatrix} \gamma_{21} & \varepsilon_{21} & \lambda_{21} & \eta_{21} \\ \gamma'_{21} & \varepsilon'_{21} & \lambda'_{21} & \eta'_{21} \\ \gamma''_{21} & \varepsilon''_{21} & \lambda''_{21} & \eta''_{21} \\ \gamma'''_{21} & \varepsilon'''_{21} & \lambda'''_{21} & \eta'''_{21} \end{bmatrix},$$

$$[K_{22}] = \begin{bmatrix} \gamma_{22} & \varepsilon_{22} & \lambda_{22} & \eta_{22} \\ \gamma'_{22} & \varepsilon'_{22} & \lambda'_{22} & \eta'_{22} \\ \gamma''_{22} & \varepsilon''_{22} & \lambda''_{22} & \eta''_{22} \\ \gamma'''_{22} & \varepsilon'''_{22} & \lambda'''_{22} & \eta'''_{22} \end{bmatrix},$$

$$[K_{32}] = \begin{bmatrix} \gamma_{32} & \varepsilon_{32} & \lambda_{32} & \eta_{32} \\ \gamma'_{32} & \varepsilon'_{32} & \lambda'_{32} & \eta'_{32} \\ \gamma''_{32} & \varepsilon''_{32} & \lambda''_{32} & \eta''_{32} \\ \gamma'''_{32} & \varepsilon'''_{32} & \lambda'''_{32} & \eta'''_{32} \end{bmatrix},$$

$$[K_{33}] = \begin{bmatrix} \gamma_{33} & \varepsilon_{33} & \lambda_{33} & \eta_{33} \\ \gamma'_{33} & \varepsilon'_{33} & \lambda'_{33} & \eta'_{33} \end{bmatrix}. \tag{10}$$

The undetermined constant C_{ij} ($i = 1,2,3$) can be obtained by solving formula (9). $j = 1,2,3,4$ and the undetermined constants are substituted back to formula (5), that is, the theoretical solution of the static uplift of each beam section at the stress stage at that time. By multiplying the theoretical solution of the static buoyancy of each beam segment by the T-hour compression reduction coefficient of the soil $[H]$, the theoretical solution of the segment buoyancy can be obtained:

$$L = \int y_i \cdot H_i dt + C_l, \tag{11}$$

where C_1 is the floating volume of the segment caused by other construction factors (including the grouting method and slurry properties) and it is a fixed constant under certain working conditions. The total uplift of the tunnel can be obtained by superposition of the vertical deformation of the tunnel obtained by the two methods.

4. Project Overview and Numerical Model Establishment

The foundation pit of the passage project crossing Xuzhou Metro Line 2 is constructed by the open cut and sequential method. The excavation area of the foundation pit is 1600 m^2, and the excavation depth is 10.8 m. The bottom of the foundation pit is only 2.4 m away from the roof of the tunnel. The soil inside and outside the foundation pit is reinforced by the MJS method, and the foundation pit is supported by the combination of the bored pile with Φ800 mm @1000 mm and the internal support. The diameter of the existing shield tunnel is 6.2 m, the thickness of the segment is 0.3 m, and the net distance between the left and right tunnels is about 8 m, as shown in Figure 4.

Considering the influence on the shield tunnel, the safety level of the foundation pit is first grade. Due to the large range of foundation pit excavation, in order to reduce the influence of the overall one-time excavation on the existing tunnel structure, the foundation pit is divided into six partitions for block excavation considering the actual working conditions, as shown in Figure 5.

The actual working condition of the site foundation pit is a parallelogram, but in order to facilitate the theoretical derivation and the convenience of the subsequent FLAC 3D modeling, the shape of the foundation pit is regularized to become a rectangle.

According to the geological survey report, the strata involved can be mainly divided from top to bottom into

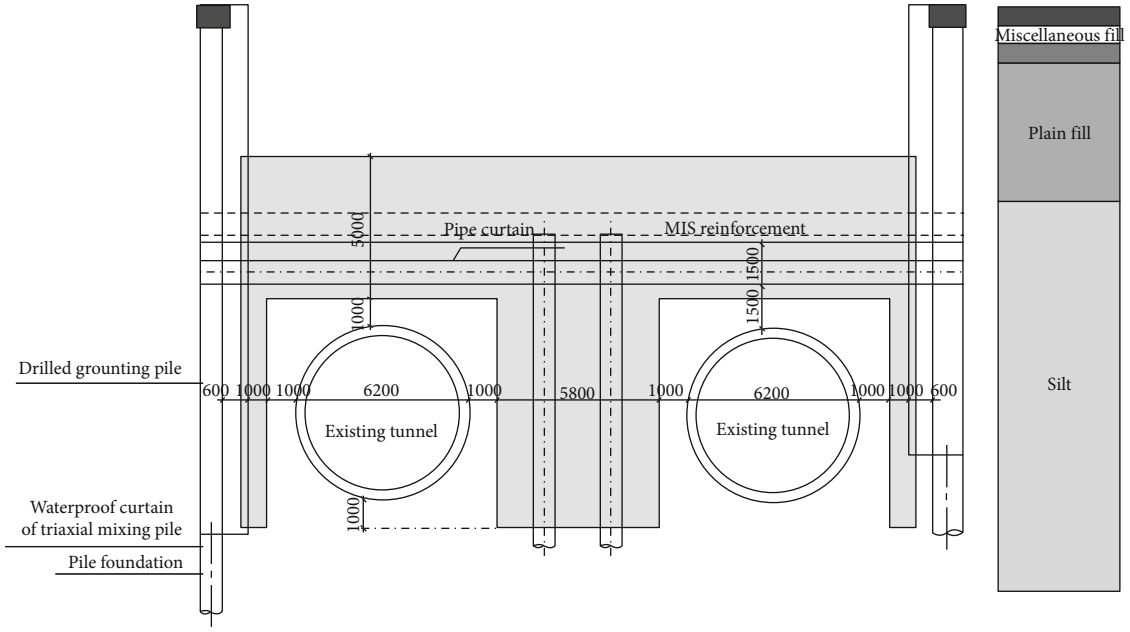

Figure 4: Vertical stratigraphic labeling on the left side of the longitudinal section of the foundation pit crossing the subway node.

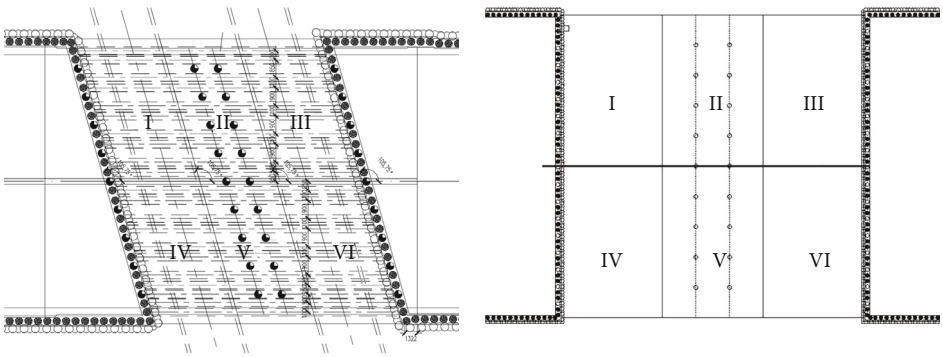

Figure 5: Construction process diagram of the foundation pit.

miscellaneous fill, plain fill, clay, silt, and moderately weathered limestone. The solid element is used for the simulation of the stratum, reinforced soil, shield segment, and pile body. The beam structural unit is used for the simulation of the support in the foundation pit, and the liner structural unit is used for the simulation of the diaphragm wall. The parameters of the constitutive model are shown in Table 1.

In order to ensure the safety of the existing subway tunnel structure, the soil around the tunnel is usually reinforced by the MJS method in the project. As presented in Figure 6, the thickness of the solid added above the tunnel is 4.5 m and the thickness of the solid added on both sides of the tunnel is 2–6 m. There is 1 m safe distance between the solid added and the tunnel. Two rows of uplift piles are set between the left and right tunnels to connect with the bottom plate of the foundation pit structure, and the length of bored piles on both sides of the tunnel is appropriately increased.

The simulation is divided into 5 analysis steps according to different construction stages: (1) applying gravity stress field, balancing ground stress, and clearing displacement; (2) excavating the tunnel soil, activating and assigning the elastic element parameters to the tunnel segment, and using the "apply nstress" command to force the surface to simulate the grouting pressure; (3) MJS reinforcement of the soil around the tunnel and construction of uplift piles; (4) foundation pit partition construction; and (5) connecting the construction structural floor with the uplift pile.

The optimal construction sequence of each partition needs to be determined after it is necessary to determine the optimal construction sequence of each zone. Zone II and zone V are suitable for the first construction because the excavation area is small and the disturbance effect on soil and surrounding existing structures is weak. The overall construction sequence of area I and area IV should be earlier than that of area III and area VI, because there are many

Table 1: Calculation parameters of the soil layer.

Soil type	Thickness (m)	Bulk modulus (MPa)	Shear modulus (MPa)	Density (kg/m^3)	Cohesion (KPa)	Friction angle (°)
Miscellaneous fill	2.2	5	3.2	1700	10	8
Plain fill	4.9	12.5	5.0	1860	21	10
Silt	13.8	16.0	8.6	1950	12	18
Clay	10.5	18.6	9	1960	75	22
Medium weathered limestone	8.6	840	490	2300	240	37

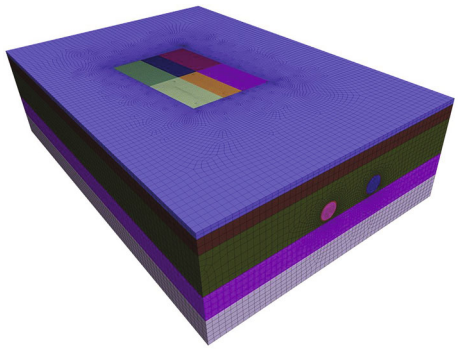

Figure 6: 3D numerical calculation model.

Table 2: Excavation sequence table and final maximum uplift value of the tunnel.

Scheme number	Excavation sequence	Tunnel maximum uplift value (mm)
1	II ⟶ V ⟶ I ⟶ VI ⟶ IV ⟶ III	12.86
2	II ⟶ I ⟶ III ⟶ V ⟶ IV ⟶ VI	12.13
3	V ⟶ II ⟶ IV ⟶ III ⟶ I ⟶ VI	13.65
4	V ⟶ IV ⟶ VI ⟶ II ⟶ I ⟶ III	13.25

buildings nearby and the surrounding environment is poor. Based on this, the different excavation sequences and the maximum uplift values of the final tunnel obtained by the above simulation analysis steps of each scheme are shown in Table 2.

It can be seen in the table that the influence of the change of the excavation sequence of the foundation pit on the deformation of the tunnel is different. The final maximum uplift value of the tunnel under scheme 2 is the smallest, and the excavation sequence of scheme 2 should be selected for foundation pit construction. The subsequent numerical simulation also selects the construction sequence under the scheme to study the deformation and stress law of the tunnel under different working conditions.

5. Calculation Results and Comparative Analysis

5.1. Tunnel Deformation Analysis without Reinforcement Measures. In order to verify and compare the vertical deformation results of the tunnel obtained by the theoretical method and to explore the weakening effect of the MJS method on the stress and deformation transfer of the soil around the tunnel, it is necessary to carry out the excavation simulation of the foundation pit without reinforcement measures. The vertical deformation of the tunnel under this condition is shown in Figure 7.

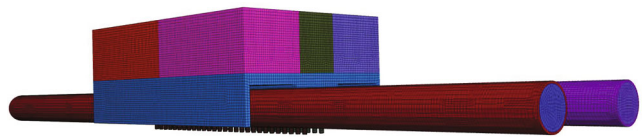

Figure 7: 3D grid division diagram of tunnel reinforcement.

The calculation shows that after the excavation of the foundation pit, the maximum uplift of the tunnel without reinforcement measures reaches 28.57 mm, which occurs in the position of the left line tunnel near the center line of the foundation pit, and the maximum uplift of the right line tunnel is 26.83 mm, which obviously exceeds the allowable deformation of the subway shield tunnel, which seriously affects the safe use and normal operation of the existing subway tunnel. Since the excavation of the upper area of the left line tunnel is earlier than that of the upper area of the right line tunnel, the uplift value of the left line tunnel is greater than that of the right line. As the position close to the center line of the foundation pit, the tunnel uplift is gradually increasing. The maximum uplift deformation of the tunnel under different construction stages is shown in Figure 8.

It is shown that the maximum uplift of the tunnel increases gradually with the construction steps. After the completion of the tunnel construction, the maximum uplift value is 7.69 mm, accounting for 26.9% of the total deformation, indicating that the grouting pressure has caused a certain amount of uplift of the segment in the tunnel shield construction. The increase of tunnel uplift caused by excavation construction in II, I, and III zones in the north of the foundation pit is 13.31 mm, which is about 1.8 times of that caused by excavation construction in V, IV, and VI zones in the south of the foundation pit. In the construction process of the north of the foundation pit, more attention should be paid to the control of tunnel deformation. In addition, in the process of foundation pit construction, due to the large excavation area and the early construction sequence, the excavation of area I has the greatest impact on the uplift value of tunnel segments. The deformation increase in this

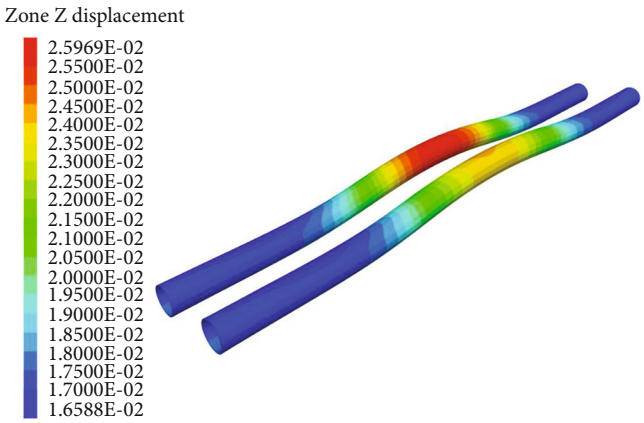

Figure 8: Cloud images of tunnel uplift deformation without reinforcement measures.

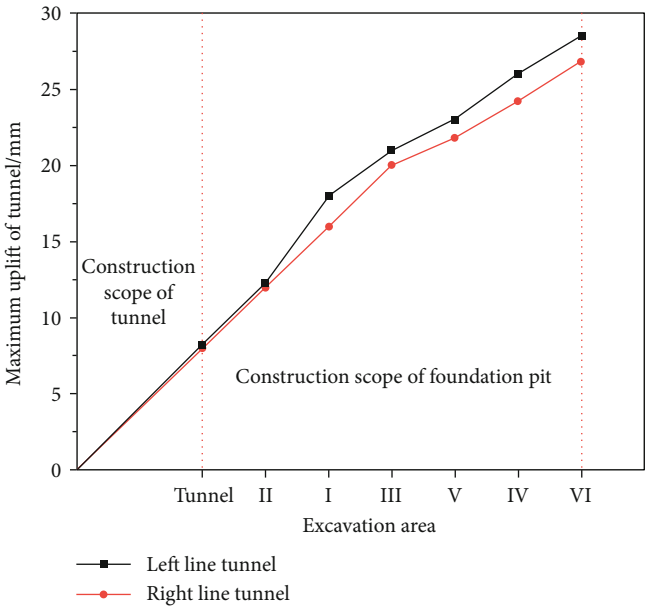

Figure 9: Maximum tunnel uplift deformation under different construction stages.

stage is 5.74 mm, accounting for about 20.1% of the tunnel uplift deformation in the whole construction process. Therefore, the reinforcement strength can be appropriately increased below this area.

5.2. Tunnel Deformation and Stress Analysis under Reinforcement Measures. In order to further study the control effect of the reinforcement method on tunnel deformation, the vertical deformation nephogram and horizontal deformation nephogram of the tunnel under the condition of reinforcement measures are extracted as shown in Figure 9.

It can be found that the uplift deformation of the tunnel is effectively limited after the reinforcement measures are taken and the maximum uplift is 12.13 mm, which is reduced by 57.84% compared with that before the reinforcement, which meets the limit displacement requirements of the subway tunnel. It shows that the MJS reinforcement has obvious control effect on the deformation of the tunnel structure. The maximum uplift position of the tunnel is transferred to the bottom of the tunnel. This is because after the reinforcement measures are taken, the uplift deformation of the tunnel is mainly caused by the grouting pressure during the shield construction of the tunnel and the excavation unloading of the tunnel itself, so that the overall floating amount below the tunnel is greater than that above. At the same time, as is known that the horizontal displacement of the tunnel is small, the maximum value is 2.35 mm, which also meets the tunnel deformation limit. The horizontal displacement of the inner part of the left and right line tunnel under the foundation pit is small due to the blocking effect of the solid and uplift pile, which verifies the effectiveness of the reinforcement scheme.

In order to further study the effect of the reinforcement scheme on the tunnel, the cloud picture of the vertical stress field around the tunnel structure at the section where the maximum deformation after foundation pit excavation is located is extracted as shown in Figure 10.

It can be seen from the analysis that in the area far from the excavation of the tunnel foundation pit, the stress distribution is still approximately linear with the soil depth and the vertical stress field of the soil around the excavation area is greatly disturbed. Under the action of the gravity of the reinforcement, the soil stress in the area below the tunnel presents a "groove type" distribution. Due to the self-weight stress of the soil transmitted by the upper structure and under the combined action of the grouting pressure, the vertical stress is slightly larger than that of the upper part and the maximum value appears at the arch waist of the tunnel.

5.3. Comparative Analysis of Calculation Results. The parameters such as grouting pressure, Poisson's ratio, and foundation pit excavation depth are substituted into formulas (3) and (11), and the cumulative buoyancy of the tunnel can be obtained by superposition of the two calculation results. In order to verify the accuracy and reliability of the theoretical calculation formula and the simulation parameters in this paper, the deformation law of the tunnel is further analyzed; therefore, the comparative curves of the tunnel uplift under the analytical calculation results, the measured results, and the numerical calculation results under the above two working conditions are drawn, as shown in Figure 11.

The theoretical values are also shown in Figure 12. It can be found that the tunnel under different calculation methods and working conditions shows a bending state of large deformation in the middle and small deformation at both ends. The curve of numerical simulation results under the condition of reinforcement measures can better fit the variation law of measured values, indicating that the value of simulation parameters and the establishment of the model are more in line with the actual working conditions. The maximum uplift deformation of the tunnel obtained by field measurement is 11.24 mm, which is 7.3% smaller than the numerical simulation results. This is because of the obvious

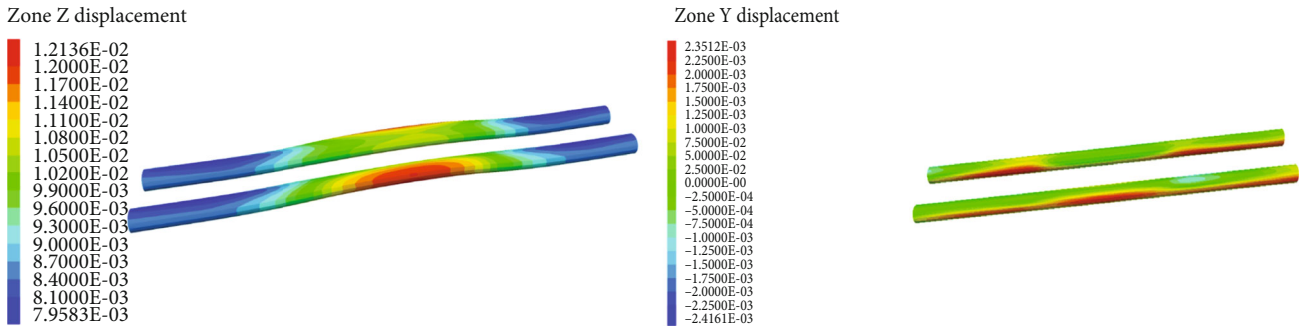

Figure 10: Tunnel deformation under reinforcement measures.

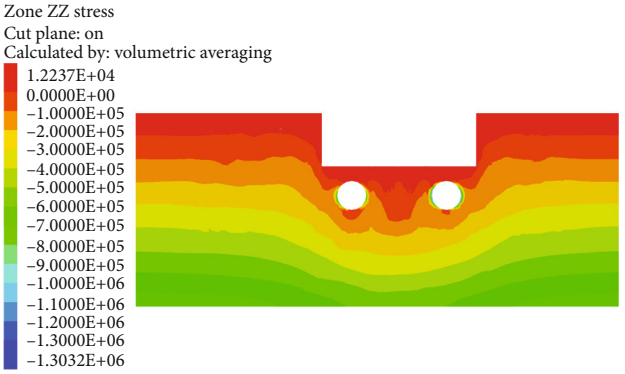

Figure 11: Vertical stress field around the tunnel structure after foundation pit excavation.

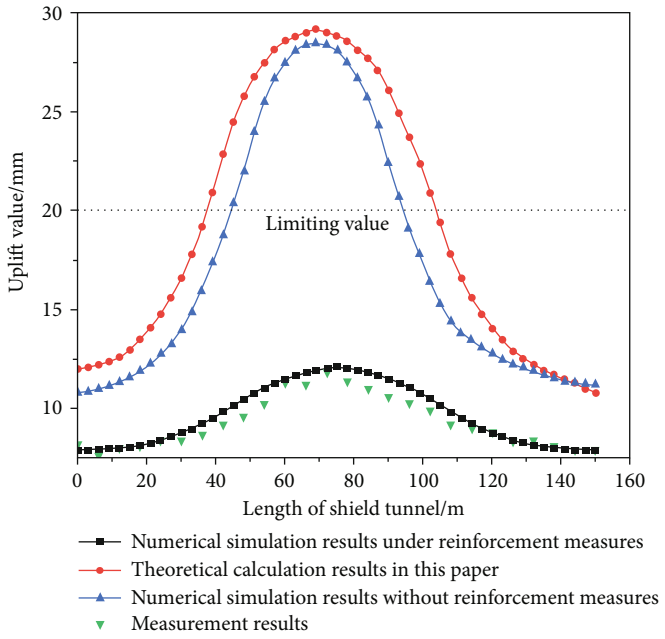

Figure 12: Comparison of tunnel uplift values obtained by different methods.

space-time effect and the looseness of the soil in the actual construction process and the influence depth of foundation pit excavation is smaller than that of the simulation. Therefore, the measured uplift is smaller than the simulation value after the reinforcement measures are taken but the variation law and value of the two values are close, indicating that the parameter value in the simulation is reasonable. From an overall perspective, the variation law of the tunnel uplift value obtained by theoretical calculation and numerical simulation under the condition without reinforcement measures is basically consistent, indicating that the theoretical calculation can better predict the deformation law of the tunnel.

Because the superposition effect of the tunnel and foundation pit construction is ignored in the theoretical calculation and the stiffness of the tunnel segment is larger in the numerical simulation, the theoretical value is slightly larger than the simulation value. The maximum uplift deformation of the tunnel obtained by the theory is 29.52 mm, and the value obtained by the simulation is 3.2% smaller than the theoretical value, indicating that the theoretical calculation results are more conducive to safety.

6. Conclusion

A theoretical calculation method is proposed to obtain the analytical solution of the floating amount of the existing shield tunnel under the superposition effect of the foundation pit and tunnel construction, which provides a more accurate prediction method for the tunnel deformation law under such projects. Through numerical simulation analysis, the deformation law of the tunnel under partition excavation and MJS reinforcement is studied and compared.

Data Availability

The data used to support the findings of this study are available from the corresponding author upon request.

Conflicts of Interest

The authors declare that there are no conflicts of interest regarding the publication of this paper.

Acknowledgments

The authors acknowledge the support received from the Natural Science Fund for Colleges and Universities in Jiangsu Province (no. 20KJA560003), China Postdoctoral Science Foundation (no. 2020M681769), and Guidance Project of Housing and Urban-Rural Development Department of Jiangsu Province (2019ZD079 and 2017ZD094). This work was also supported by the Qing Lan Project and Postdoctoral Workstation of Hefei, as well as the JiangSu Collaborative Innovation Center for Building Energy Saving and Construction Technology (Grant: SJXTBS1710) and Xuzhou Science and Technology Project (Grant: KC18133).

References

[1] Z. G. Zhang, M. S. Huang, and W. D. Wang, "Evaluation of deformation response for adjacent tunnels due to soil unloading in excavation engineering," *Tunnelling and Underground Space Technology Incorporating Trenchless Technology Research*, vol. 38, pp. 244–253, 2013.

[2] J. S. Sharma, A. M. Hefny, J. Zhao, and C. W. Chan, "Effect of large excavation on deformation of adjacent MRT tunnels," *Tunnelling and Underground Space Technology Incorporating Trenchless Technology Research*, vol. 16, no. 2, pp. 93–98, 2001.

[3] X. Wen and C. R. Pang, "Influence of foundation pit excavation on existing shield tunnel and its protection range," *Applied Mechanics & Materials*, vol. 580-583, pp. 1258–1263, 2014.

[4] M. Devriendt, L. Doughty, P. Morrison, and A. Pillai, "Displacement of tunnels from a basement excavation in London," *Proceedings of the Institution of Civil Engineers*, vol. 163, no. 3, pp. 131–145, 2010.

[5] C. Jing, G. W. Qian, and H. X. Zuo, "Analysis for influence of excavation on adjacent existing shield tunnel," in *Proceedings of the 2016 4th International Conference on Mechanical Materials and Manufacturing Engineering*, Wuhan, People's Republic of China, 2016.

[6] J. T. Qiu, J. Jiang, X. J. Zhou, Y. F. Zhang, and Y. D. Pan, "Analytical solution for evaluating deformation response of existing metro tunnel due to excavation of adjacent foundation pit," *Journal of Central South University*, vol. 28, no. 6, pp. 1888–1900, 2021.

[7] D. M. Zhang, X. C. Xie, Z. L. Li, and J. Zhang, "Simplified analysis method for predicting the influence of deep excavation on existing tunnels," *Computers and Geotechnics*, vol. 121, no. 2, article 103477, 2020.

[8] J. W. Liu, C. H. Shi, and M. F. Lei, "Analytical method for influence analysis of foundation pit excavation on underlying metro tunnel," *Journal of Central South University: Science and Technology*, vol. 50, no. 9, pp. 2215–2225, 2019.

[9] S. Q. Yan, C. H. Qiu, and J. F. Xu, "Numerical simulation of a deep excavation near a shield tunnel," *Tehnički vjesnik*, vol. 25, 2018.

[10] S. H. Ye and Z. H. Zhao, "Deformation analysis and safety assessment of existing metro tunnels affected by excavation of a foundation pit," *Underground Space*, vol. 6, no. 4, pp. 421–431, 2021.

[11] Z. T. Yu, H. Y. Wang, and W. J. Wang, "Experimental and numerical investigation on the effects of foundation pit excavation on adjacent tunnels in soft soil," *Mathematical Problems in Engineering*, vol. 2021, 11 pages, 2021.

[12] S. Y. Fan, Z. P. Song, and T. Xu, "Tunnel deformation and stress response under the bilateral foundation pit construction: a case study," *Engineering*, vol. 21, no. 3, p. 77, 2021.

[13] J. S. Ding, Y. Q. Xian, and T. J. Liu, "Study on the influence of the shield tunnel deformation due to excavation of foundation pit with field data," *Advanced Materials Research*, vol. 16, no. 3, pp. 446–449, 2012.

[14] Y. Gui, Z. Zhao, and X. Qin, "Study on deformation law of deep foundation pit with the top-down method and its influence on adjacent subway tunnel," *Advances in Civil Engineering*, vol. 2020, no. 8, p. 15, 2020.

[15] X. H. Zhang, G. Wei, and C. W. Jiang, "The study for longitudinal deformation of adjacent shield tunnel due to foundation pit excavation with consideration of the retaining structure deformation," *Deformation*, vol. 12, no. 12, p. 2103, 2020.

[16] Y. Jiang, "Influence on metro tunnel structure caused by foundation pit excavation considering coupling effect," *Fresenius Environmental Bulletin*, vol. 17, no. 4, 2019.

[17] X. M. Zhang, X. F. Ou, J. S. Yang, and J. Y. Fu, "Deformation response of an existing tunnel to upper excavation of foundation pit and associated dewatering," *International Journal of Geomechanics*, vol. 17, no. 4, 2017.

[18] A. M. Hefny, H. C. Chua, and J. Zhao, "Parametric studies on the interaction between existing and new bored tunnels," *Tunnelling and Underground Space Technology*, vol. 19, no. 4-5, p. 471, 2004.

[19] X.-L. Tao, Y.-H. Su, Q.-Y. Zhu, and W.-L. Wang, "Pasternak model-based tunnel segment uplift model of Subway shield

tunnel during construction," *Advances in Civil Engineering*, vol. 2021, no. 5, p. 10, 2021.

[20] R. Liang, T. Xia, M. Huang, and C. Lin, "Simplified analytical method for evaluating the effects of adjacent excavation on shield tunnel considering the shearing effect," *Computers and Geotechnics*, vol. 81, no. 3, pp. 167–187, 2017.

[21] Y. Tan, X. Li, Z. Kang, J. Liu, and Y. Zhu, "Zoned excavation of an oversized pit close to an existing metro line in stiff clay: case study," *Journal of Performance of Constructed Facilities*, vol. 29, no. 6, 2014.

[22] H. Sun, Y. Chen, J. Zhang, and T. Kuang, "Analytical investigation of tunnel deformation caused by circular foundation pit excavation," *Computers and Geotechnics*, vol. 106, no. 5, pp. 193–198, 2019.

[23] K. C. Shu and N. Xiong, "Research on strong agile response task scheduling optimization enhancement with optimal resource usage in green cloud computing," *Future Generation Computer Systems*, vol. 124, pp. 12–20, 2021.

[24] W. Shu, K. Cai, and N. N. Xiong, "A ShortTerm traffic flow prediction model based on an improved gate recurrent unit neural network," *IEEE Transactions on Intelligent Transportation Systems*, pp. 1–12, 2021.